

Article

Ecotoxicity of 2,4-Dichlorophenol to *Microsorium pteropus* by High Spatial Resolution Mapping of Stoma Oxygen Emission

Ning Zhong^{1,2,3} and Daoyong Zhang^{1,4,*}

¹ State Key Laboratory of Desert and Oasis Ecology, Xinjiang Institute of Ecology and Geography, Chinese Academy of Sciences, Urumqi 830011, China; zhong-ning@163.com

² Fujian Province Key Laboratory of Modern Analytical Science and Separation Technology, College of Chemistry, Chemical Engineering & Environmental Science, Minnan Normal University, Zhangzhou 363000, China

³ University of Chinese Academy of Sciences, Beijing 100049, China

⁴ Key Laboratory of Microbial Technology for Industrial Pollution Control of Zhejiang Province, College of Environment, Zhejiang University of Technology, Hangzhou 310014, China

* Correspondence: zhang-daoyong@163.com; Tel./Fax: +86-991-7885446

Abstract: The toxicity of emerging organic pollutants to photosystems of aquatic plants is still not well clarified. This study aimed to develop a novel ecotoxicological experimental protocol based on nanoscale electrochemical mapping of photosynthetic oxygen evolution of aquatic plants by scanning electrochemical microscopy (SECM). The protocol was also checked by confocal laser scanning microscopy (CLSM), the traditional Clark oxygen electrode method, and the chlorophyll fluorescence technique. The typical persistent organic pollutant 2,4-dichlorophenol (2,4-DCP) in a water environment and the common aquatic *Microsorium pteropus* (*M. pteropus*) were chosen as the model organic pollutant and tested plant, respectively. It was found that the SECM method could discriminate the responses of stoma micromorphology and spatial patterns of photosynthetic oxygen evolution on single stoma well. The shape of stoma blurred with increasing 2,4-DCP concentration, which was in good agreement with the CLSM images. The dose–response curves and IC₅₀ values obtained from the SECM data were verified by the data measured by the traditional Clark oxygen electrode method and chlorophyll fluorescence test. The IC₅₀ value of single-stoma oxygen emission of plant leaves exposed for 24 h, which was derived from the SECM current data (32,535 µg L⁻¹), was close to those calculated from the maximum photosynthetic efficiency (F_v/F_m) measured by the chlorophyll fluorescence test (33,963 µg L⁻¹) and the Clark oxygen electrode method photosynthetic oxygen evolution rate (32,375 µg L⁻¹). The 72 h and 96 h 2,4-DCP exposure data further confirmed the reliability of the nanoscale stoma oxygen emission mapping methodology for ecotoxicological assessment. In this protocol, the procedures for how to collect effective electrochemical data and how to extract useful information from the single-stoma oxygen emission pattern were well established. This study showed that SECM is a feasible and reliable ecotoxicological tool for evaluation of toxicity of organic pollutants to higher plants with a unique nanoscale visualization advantage over the conventional methods.

Keywords: scanning electrochemical microscopy; chlorophyll fluorescence; dose–response curve; photosynthetic oxygen evolution; nanoscale mapping; persistent organic pollutants



Citation: Zhong, N.; Zhang, D. Ecotoxicity of 2,4-Dichlorophenol to *Microsorium pteropus* by High Spatial Resolution Mapping of Stoma Oxygen Emission. *Water* **2024**, *16*, 1146. <https://doi.org/10.3390/w16081146>

Academic Editor: Massimo Zacchini

Received: 2 March 2024

Revised: 1 April 2024

Accepted: 4 April 2024

Published: 18 April 2024



Copyright: © 2024 by the authors. Licensee MDPI, Basel, Switzerland. This article is an open access article distributed under the terms and conditions of the Creative Commons Attribution (CC BY) license (<https://creativecommons.org/licenses/by/4.0/>).

1. Introduction

Photosynthesis plays an important role in agricultural production and the global carbon cycle. But the photosynthesis organ of plants is highly sensitive to the toxicity of organic pollutants and the toxic effects of pollutants on photosynthesis are usually probed by chlorophyll fluorescence and oxygen evolution rate [1–3]. Measurement of the photosynthetic oxygen evolution rate of plants under stress, which directly indicates the toxicity of pollutants to the oxygen evolution complex, is performed by a Clark oxygen

electrode in a thermostatic closed chamber at a constant temperature [4]. This conventional electrochemical method, however, cannot probe oxygen emission at a single-stoma level and cannot give the spatial distribution of oxygen concentration in and around the stoma, which is sometimes important for understanding the responses of plants to environmental stresses. Although net photosynthesis can be estimated by gas exchange and photosynthetic electron transport can be estimated by non-invasive measurements of chlorophyll fluorescence, the measurement scale is relatively large, yielding gross measurements from square centimeters of plant tissue [5,6]. For plant leaves, the density of the chloroplasts may affect the measurement results. One can standardize the readings to a 'per chloroplast' or single cell measurements, or one can seek alternative methods that are less affected by organelle density [7]. Because many functions of living cells and tissues are tightly related to photosynthesis, it is desirable to measure the effects of organic pollutants on photosynthetic reactions and the spatial distribution of oxygen concentration in and around the stoma in small-scale measurements and non-invasively.

The technique of scanning electrochemical microscopy (SECM) is often used to characterize chemical processes and spatial morphological features of the substrate when the tip is moved near the surface of a conductive or insulating bottom substrate in solution in which the current flows through an ultramicroelectrode (UME) [8].

The SECM tip can be moved at Å resolution so that the chemical concentration and morphology of the conductive or insulating bottom substrate surface can be imaged at atomic resolution when the tip is scanned in the X-Y plane at a constant height [9]. SECM has the potential to examine the response of photosynthetic oxygen evolution under environmental stresses because oxygen produced by the water splitting center in photosystem II is a mediator that can be reliably probed by UMEs [10]. Since oxygen is released from the stoma during photosynthesis, SECM can simultaneously map the oxygen concentration distribution and structure of stoma, which provide complementary data for the traditional liquid oxygen electrode method and chlorophyll fluorescence tests. Very limited studies showed the application potential of SECM for this purpose. Tsionsky et al. [11] firstly monitored photoelectrochemistry and in vivo topography of single stoma in stress-free *Tradescantia fluminensis* Vell cv. Variegata by using SECM. Zhu et al. [12] firstly used an SECM probe to detect oxygen evolution and the changes to individual stoma structure in *Brassica juncea* (L.) Czern. cv. AC Vulcan (Indian mustard) caused by Cd stress. Besides its powerful function and extensive application in the field of biology [13], SECM has not been systemically verified for probing toxic effects of pollutants from the perspective of ecotoxicology. The relevant protocols to obtain reproducible and reliable ecotoxicological data are still unavailable. Some problems must be solved before it is accepted by ecotoxicologists. For example, in the published literature, the leaf disc system for SECM detection is bubbled by air to ensure enough CO₂ in water for photosynthesis. However, the CO₂ content in water can be significantly affected by temperature, air pressure, and bubbling time and efficiency. The CO₂ in water after aeration may not be enough to maintain maximum photosynthesis performance for long-time SECM measurement. In addition, only one pollutant concentration was set in their experiments to probe the toxicity of the pollutant, which cannot meet the requirement of the dose–response relationship in ecotoxicological experimental design and the toxicological indices, such as the dose–effect curve, and the half maximal inhibitory concentration (IC₅₀) cannot be estimated.

2,4-dichlorophenol (2,4-DCP) has been listed by the U.S. Environmental Protection Agency as a priority control pollutant because of its potential carcinogenicity and its high toxicity even at a low concentration [14–17]. 2,4-DCP mainly arises from the extensive use of pesticides, herbicides, and fungicides [18]. However, the mechanisms of 2,4-DCP toxicity on leaf photosynthetic reactions have not yet been firmly established. The mechanisms of 2,4-DCP-induced changes in stomata are also not well understood.

M. pteropus is a common higher freshwater aquatic plant which has high demand for ornamentation and is often used as a water pollution indicator [19]. *M. pteropus* was chosen as the test material because previous research has shown that its multiple sites

in PSII and PSI are highly sensitive to heavy metal exposure [1,20,21]. However, studies on the photosynthetic toxicity of *M. pteropus* plants under organic pollution stress are still rare. Because 2,4-DCP is a major organic pollutant in water bodies, hydrophytes such as *M. pteropus* are frequently exposed to 2,4-DCP. So, simultaneous quantification measurements of toxicity of PSI and PSII activities and mapping of the spatial distribution of photosynthetic oxygen evolution under stress of 2,4-DCP are needed in order to obtain more accurate information about effects of 2,4-DCP on photosynthetic apparatus.

The aim of the present study was to develop a reproducible experimental protocol for assessment of the ecotoxicity of 2,4-DCP exposure to *M. pteropus* based on nanoscale SECM visualization and quantification of photosynthetic oxygen evolution at the single-stoma level. The stoma structure upon exposure to 2,4-DCP treatment was simultaneously imaged and compared with those obtained by CLSM. The dose–response curve and derived IC_{50} were comparatively verified by the chlorophyll fluorescence method and the traditional Clark liquid oxygen electrode method.

2. Materials and Methods

2.1. Plant Materials

M. pteropus (wild type) [22] seedlings were purchased from a market in Urumqi of China and cultivated in a glass aquarium (length 500 mm, width 300 mm, height 550 mm) filled with tap water at 25 ± 2 °C under irradiance of $100 \mu\text{mol photons m}^{-2}\text{s}^{-1}$ with a 12/12 h light/dark photoperiod [1]. Then, the seedlings were taken out from the glass aquarium after 4 d of adaptation of the culture. The healthy seedlings without spores and dark spots, about 25 ± 2 cm in height, were selected for toxicological tests.

2.2. Chemicals

All chemicals used in this study were at least of analytic grade. The 2,4-DCP solutions were prepared by dissolving solid 2,4-DCP (99%, CAS#120-83-2, Sigma-Aldrich, St. Louis, MO, USA, 105953-100G, HPLC: suitable) in tap water. Despite the 2,4-DCP guide levels for surface waters and drinking water established by regulatory organizations, higher concentrations than those suggested are frequently found in contaminated environments. In fact, reported levels of 2,4-DCP were found to be up to 50 times greater than allowable limits [16,23,24]. So, in order to ensure that the concentration range used overlaps with an environmentally relevant range, and combined with the concentration settings reported in some literature reports, the nominal concentration level gradients for 2,4-DCP treatment are set to 0.00, 0.01, 0.05, 0.1, 0.5, 1.0, 5.0, 10.0, 25.0, 50.0, 100.0, and 250.0 mg L^{-1} . The actual concentrations of 2,4-DCP in tap water was measured by high-performance liquid chromatography (HPLC, 890-0203 HITACHI, Hitachi, Tokyo, Japan) [25] which were 0.01, 0.05, 0.10, 0.48, 1.00, 4.50, 9.53, 24.90, 49.81, 92.44, and 248.53 mg L^{-1} , respectively. The chromatographic conditions are: C18 reversed-phase column (ZORBAX SB-C18, 250 mm \times 4.6 mm, 5 μm ; Agilent, Santa Clara, CA, USA); mobile phase: methanol: water, volume ratio is 60:40; flow rate: 0.8 mL min^{-1} ; column temperature: 30 °C; injection volume: 20 μL ; detection wavelength is 280 nm. 2,4-DCP concentration in the tap water was not detected.

2.3. Ecotoxicity Exposure Experiments

Twelve groups of seedlings with three seedlings in each group were transferred to twelve 500 mL cylindrical glass cylinders (355 mm \times 50 mm) containing 600 mL tap water with different measured concentrations of 2,4-DCP (0–248.53 mg L^{-1}). The seedlings grown in the tap water without addition of 2,4-DCP were used as the control. During the cultivation, some tap water was irregularly added to the cylinders to compensate the loss of water due to evaporation. All the tap water stood for at least 24 h before use in order to reduce or remove the disinfection substances. Control and 2,4-DCP stress treatments both included four replicates (each replicate containing three seedlings, i.e., $n = 4 \times 3 = 12$). Leaves of the seedlings exposed to 2,4-DCP for 24 h, 72 h, 96 h were used for SECM oxygen

emission mapping, CLSM observation, chlorophyll fluorescence test, and photosynthetic oxygen evolution rate measurement by the Clark oxygen electrode.

2.4. Stoma Oxygen Mapping by SECM

All stoma oxygen mapping and quantification were performed with an SECM workstation (920D, CH Instruments, Austin, TX, USA). The SECM instrument included three major constituent parts: the positioning system, the electrochemical system, and the active data acquisition system. In general measurement, a potential was added to the SECM probe and a current was detected by the electrochemical system [12]. The positioning system was used to displace the probe, and the data acquisition system was used to record the current and position data simultaneously. The electrochemical and positioning systems were built together in a Faraday cage to isolate external electrical noise. A well-polished 10 μm diameter platinum UME with RG 10 (HEKA Elektronik Dr. Schulze GmbH, Lambrecht, Germany) was used as the SECM tip. Reliability of the UME was checked by capacitive current and steady-state current tests. A 0.5 mm platinum wire and Ag/AgCl were used as the counter electrode and the reference electrode, respectively. In the voltammetry curve tests to characterize the electrodes, a 10 μm diameter Pt UME as a working electrode versus an Ag/AgCl reference electrode were simultaneously immersed in the solution of supporting electrolyte (containing 0.1 M KCl and 1.0 mM ferrocenemethanol).

All SECM experiments were performed at constant height mode at 25 ± 2 °C. The leaf disc at the bottom of the electrochemical cell was illuminated under 100 $\mu\text{mol photons m}^{-2}\text{s}^{-1}$ by a LED lamp. After 10 min of dark adaptation of the leaf disc to be tested, the LED lamp was turned on and SECM measurement started. A phosphate buffered saline (PBS, pH 6.86) solution containing 0.1 M NaHCO_3 was used as the supporting electrolyte which could provide excessive CO_2 for photosynthesis during measurement.

Before starting the test, a leaf disc (8 mm in diameter) was taken from *M. pteropus* seedlings with a punch. Then, the leaf disc was placed centrally at the bottom of the Teflon cylinder electrochemical cell and fixed with a round piece of transparent glass (34 mm in diameter, 4 mm in thickness) with a round hole (6 mm in diameter). The cylinder (diameter 34.8 mm, depth 22 mm) made of optically transparent polystyrene was used as an electrochemical cell with a flat bottom of uniform thickness. All the tested leaves were adapted in the dark for 10 min before being transferred to the electrochemical cell.

In probe approach experiments, the SECM tip was positioned over the leaf disc and immobilized at a distance (generally 10–15 μm) above the substrate, and then was moved down to obtain the approach curves and the tip scanning height of the subsequent mapping experiments (about 1.5 μm). The current versus the moving distance toward the leaf was measured at the UME, which was biased at a potential (−0.6 V) to obtain a steady-state current for the reduction of oxygen in the solution. The destination normalized current (the ratio of actual tip current, i_T to $i_{T\infty}$) was set gradually to a low value (e.g., 0.6) to avoid crushing the tip.

In the scanning mapping experiments, the electrode was immediately scanned at a constant height (1.5 μm above the leaf disc) after probe approach experiments. Firstly, an area of 200×200 μm (no leaf vein) of the leaf disc was scanned at a relatively faster speed (150 $\mu\text{m s}^{-1}$) to find several stomas. Then, a 100×100 μm area containing one stoma was scanned at high spatial resolution (50 $\mu\text{m s}^{-1}$) to obtain a microscale image. The current of the stoma longitude perpendicular cross-sectional line and the peak current of each stoma center were extracted. After each test, the UME was washed under ultrasonic irradiation twice and rinsed with deionized water several times, then checked with an optical microscope (IX71, Olympus Co., Tokyo, Japan) prior to use for further experiments.

2.5. Three Conventional Ecotoxicological Assessment Methods

Autofluorescence imaging of leaf disc: The autofluorescence (excited by a 488 nm laser) of the leaf discs treated with various concentrations of 2,4-DCP was observed and imaged using a CLSM (FV1000, Olympus Co., Tokyo, Japan).

Measurement of photosynthetic oxygen evolution rate: The photosynthetic oxygen evolution rates of the leaf discs treated with various concentrations of 2,4-DCP were measured using a Clark oxygen electrode (Oxygraph, Hansatech Instruments, Pentney, UK). The reaction chamber was filled with 2.0 mL PBS (pH 6.86) solution containing 0.1 M NaHCO_3 . The measurements were performed at 25 °C under 100 $\mu\text{mol photons m}^{-2}\text{s}^{-1}$ irradiance. The measured photosynthetic oxygen evolution rate was converted to the rate of oxygen release per minute of the leaf ($\text{nmol cm}^{-2} \text{min}^{-1}$).

Chlorophyll fluorescence test: The maximal PS II quantum yields (F_v/F_m) of the leaf discs treated with various concentrations of 2,4-DCP were measured by a double modulation chlorophyll fluorometer (Dual-PAM-100 system, Heinz Walz GmbH, Effeltrich, Germany). The chlorophyll fluorescence test was performed after the leaf discs were adapted in the dark for 5 min [1,26].

2.6. Calculation and Statistics

Each 2,4-DCP stress treatment was carried out in quadruplicate (three seedlings each). Means and standard deviations (SDs) were calculated using Microsoft Excel 2016. Plottings were performed with OriginPro 9.0. The best-fit values and the 95% confidence intervals of IC_{50} values were estimated by a 'normalized response-variable slope' (GraphPad Prism 5) through the mean, SD, and N (calculated with Microsoft Excel 2016 in advance). The statistical significance between 2,4-DCP treatments and control treatment was examined by one-way ANOVA (SPSS V21.0) through the least significant difference (LSD) test. The statistical significance of IC_{50} values among SECM, Clark oxygen electrode, and chlorophyll fluorescence data was examined by one-way ANOVA (SPSS V21.0) through Duncan's multiple range test (DMRT).

3. Results

3.1. SECM Mappings of Stoma Oxygen Emission

The typical $100 \times 100 \mu\text{m}$ spatial distribution images of oxygen concentration current above an individual stoma of the leaf discs (8 mm in diameter) of 2,4-DCP-treated and untreated *M. pteropus* recorded by SECM are shown in Figure 1.

Each image was obtained at $50 \mu\text{m s}^{-1}$ ($n = 12$). The probe-to-substrate distance, d , was initially set at $1.5 \mu\text{m}$. The UME was biased at -0.60 V . The electrolyte solution was PBS solution (pH 6.86) containing 0.1 M NaHCO_3 . In each image, relatively high concentrations of oxygen are deep blue to green; raised topographical features are yellow to red.

The area around the stoma was dominated by green and blue for the control and the samples treated with lower concentrations, then it gradually turned to green, yellow, and red as 2,4-DCP concentration increased up to nearly $100\text{--}250 \text{ mg L}^{-1}$, indicating the oxygen concentration in the stoma decreased with increasing 2,4-DCP concentrations. There were clear three-tined-fork-shaped stoma for the control and the samples treated with up to about 50 mg L^{-1} . However, when the concentration of 2,4-DCP continued to increase to 250 or 500 mg L^{-1} , the outline of the three-tined-fork-shaped stoma became increasingly blurred. These results were in good agreement with the CLSM fluorescence images of the stroma (Figure 2). The stomatal oxygen release concentration gradually decreased with the exposure time, which is consistent with the variation rule (Figure 2).

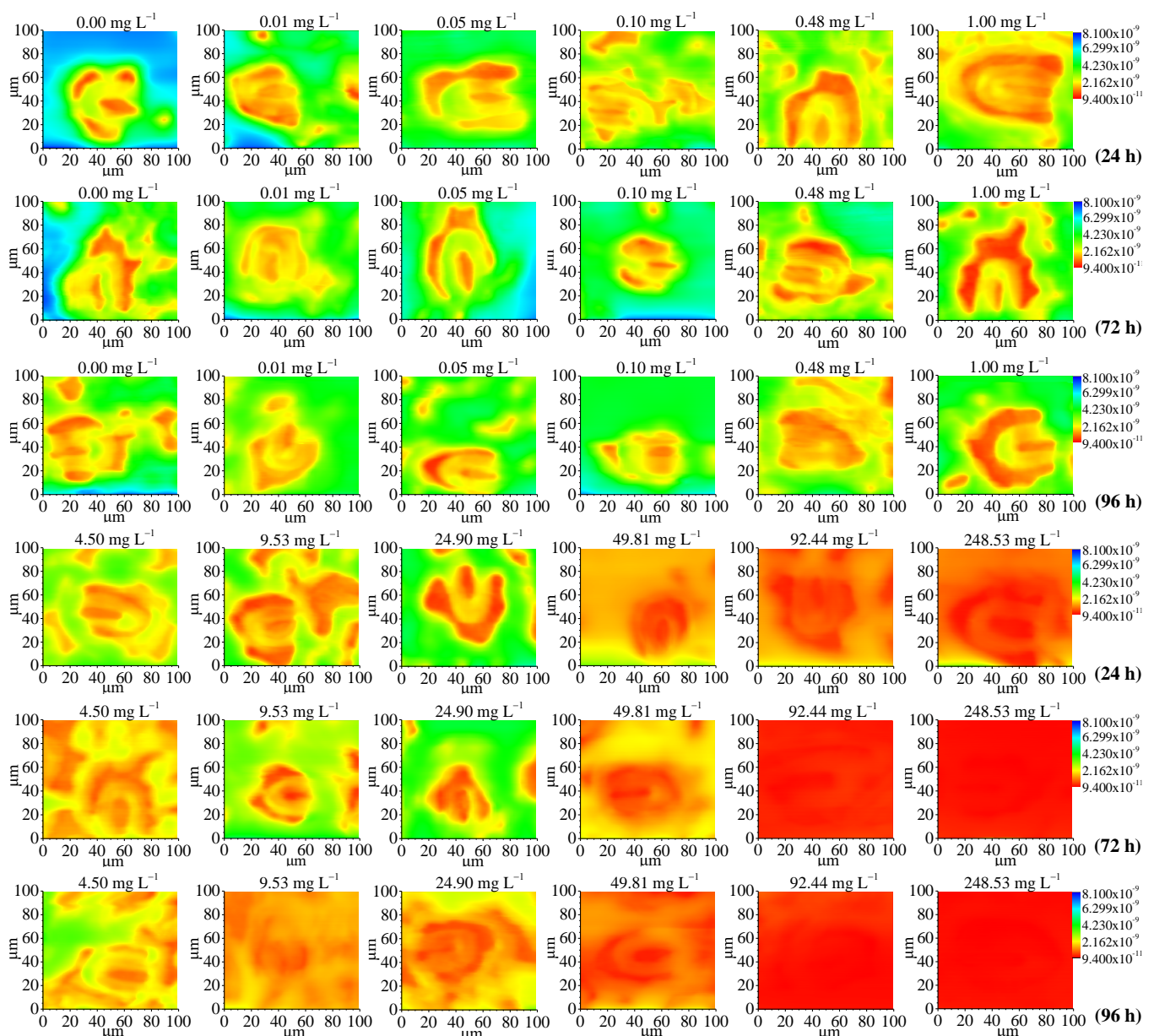


Figure 1. SECM images of *M. pteropus* stoma under various concentrations of 2,4-DCP after different times (24 h, 72 h, and 96 h).

3.2. CLSM Images of *M. pteropus* Stoma

CLSM images (at 488 nm) of *M. pteropus* stomata under various concentration of 2,4-DCP are shown in Figure 2. The concentrations of 2,4-DCP are given in the legend. The scale bar indicates 100 μm . Figure 2 shows that the stoma changed from clear and intact to blurry and damaged with increasing 2,4-DCP concentration ($n = 12$). The boundaries between the stomata and the surrounding tissues were clear in the stoma and mesophyll tissue of the control and the samples treated with lower concentrations, the stoma density was relatively evenly distributed, and the brightness was more obvious.

However, when the concentration of 2,4-DCP continued to increase to 100–250 mg L^{-1} , the degree of damage in the leaves was deepened, and black spots and black holes appeared in the leaf tissue. Meanwhile, the outline of the stoma itself and the boundary between stomata and tissue became increasingly blurred (Figure 2). These results are also consistent with the image results of the SECM with corresponding concentrations in Figure 1.

In addition, the CLSM results also confirmed that the toxicity and damage of 2,4-DCP to the stomata of *M. pteropus* also increased as the concentrations increased and the culture time prolonged.

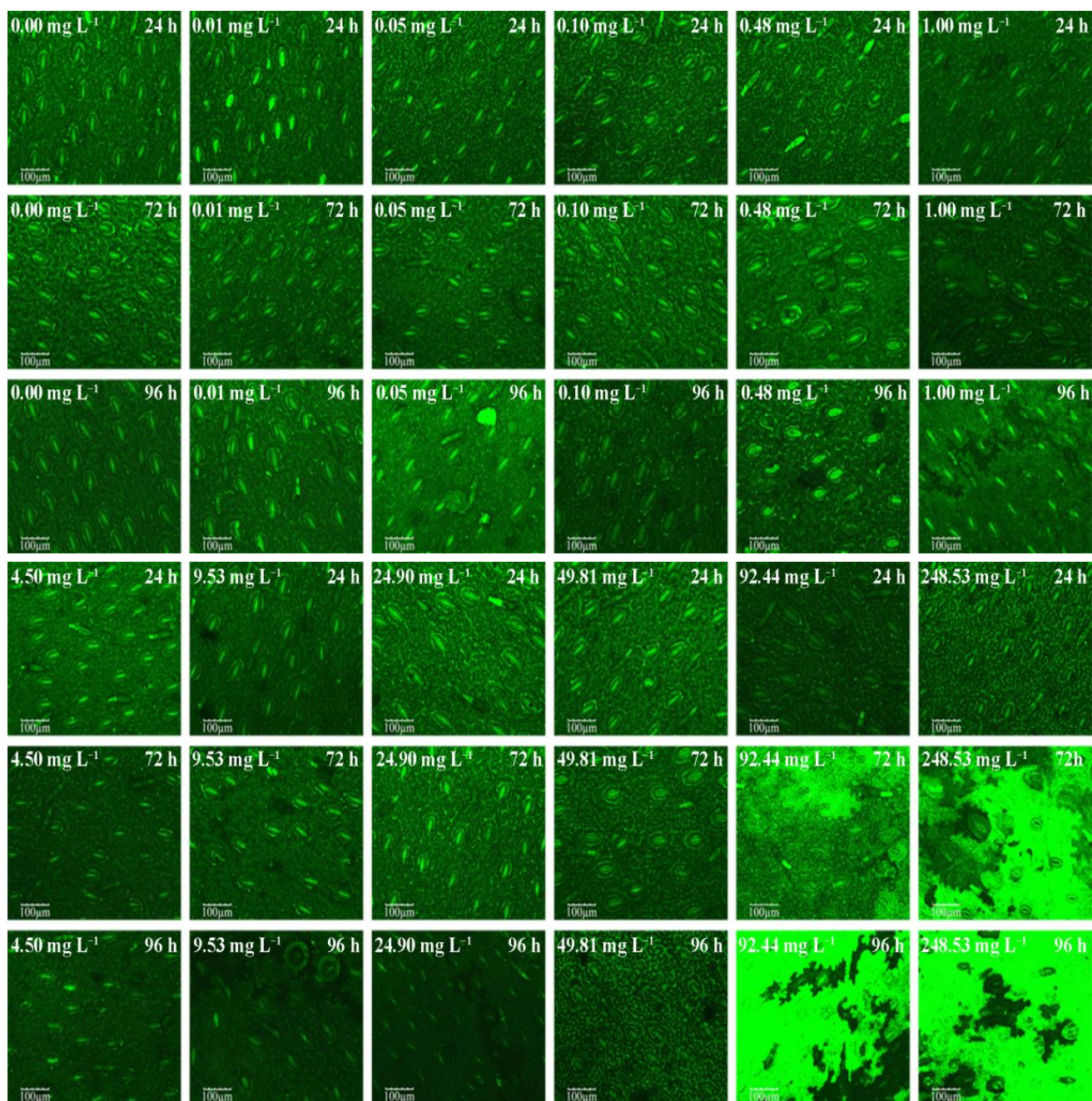


Figure 2. CLSM images of *M. pteropus* stoma under various concentrations of 2,4-DCP after different times (24 h, 72 h, and 96 h).

3.3. Estimation of IC_{50} from SECM and Other Methods

Figure 3 shows the current profile curves (a1, a2, a3), the current curves of the stoma center (b1), the photosynthetic oxygen evolution rate curves (c), the F_v/F_m curves (e), and their corresponding dose–effect curves (contain IC_{50} value) (b2, d, f) of *M. pteropus* stomata under various concentrations of 2,4-DCP for 24 h, 72 h, and 96 h. The IC_{50} value was calculated by GraphPad Prism 5 software.

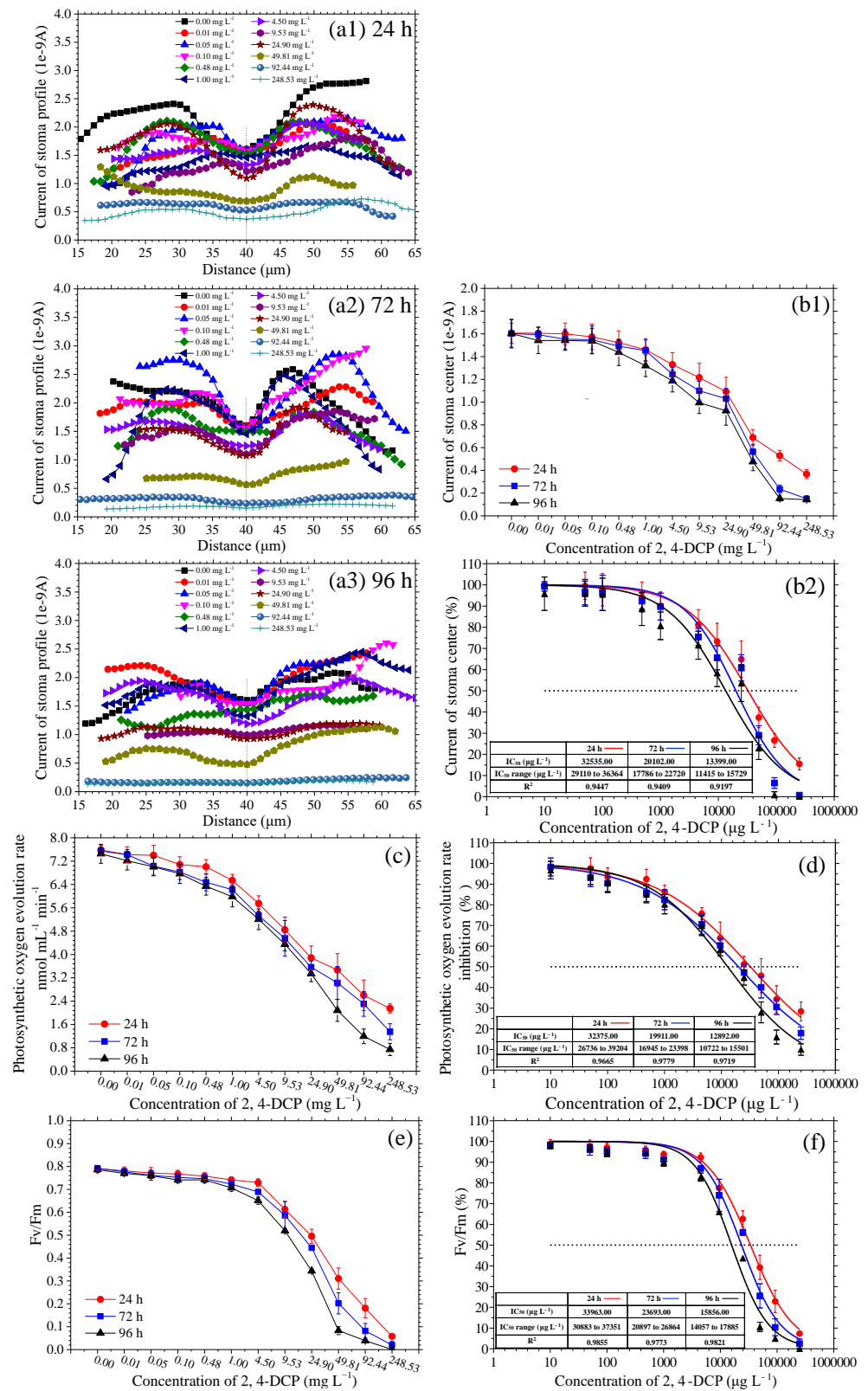


Figure 3. The current profile curves (a1–a3), the current curves of stoma center (b1), the photosynthetic oxygen evolution rate curves (c), the Fv/Fm curves (e), and their corresponding dose–effect curves (contain IC₅₀ value) (b2,d,f) of *M. pteropus* stoma under various concentrations of 2,4-DCP for 24 h, 72 h, and 96 h. The error bars represent standard deviation. Each treatment was replicated four times ($n = 12$).

Figure 3(a1–a3) shows the typical current curve along a line section of one stoma perpendicular to longitude. Oxygen concentration current at the center of the stoma was used to estimate IC_{50} because oxygen is directly emitted from the stoma core with the least influence of other factors. In order to estimate the validity of the IC_{50} derived from the oxygen concentration current from SECM data, the IC_{50} was also calculated from photosynthetic oxygen evolution data collected by the Clark liquid-phase electrode and the Fv/Fm.

It can be seen from Figure 3(b1,c,e) that oxygen concentration current at the center of the stoma, the photosynthetic oxygen evolution rate, and the Fv/Fm gradually decreased as the concentrations of 2,4-DCP increased. We found Figure 3(b2,d,f) that the best-fit values of the IC_{50} curve fit a reverse S-shape, and the IC_{50} value of by SECM is close to the IC_{50} value obtained by the photosynthetic oxygen evolution rate and the Fv/Fm.

The very close statistical significance of the IC_{50} value between the SECM method and two traditional measurement methods (Clark oxygen electrode and PAM) through the DMRT ($p = 0.949 > 0.05$) illustrated that there was no significant difference between the results obtained by the SECM method and that obtained by the two traditional methods (Table 1). In other words, the determination of the SECM method is reliable and it can introduced into the ecotoxicology field.

Table 1. Comparison of IC_{50} values obtained by three different measurement methods of *M. pteropus* treated with 2,4-DCP for different times ($\mu\text{g L}^{-1}$).

| Time | | Fv/Fm (by Dual-PAM-100) | Stomatal Center Current Value (by SECM) | Photosynthetic Oxygen Evolution Rate (by Oxygraph) |
|------|--|----------------------------|---|--|
| 24 h | IC_{50} ($\mu\text{g L}^{-1}$) | 33,963 | 32,535 | 32,375 |
| | IC_{50} range ($\mu\text{g L}^{-1}$) | 30,883 to 37,351 | 29,110 to 36,364 | 26,736 to 39,204 |
| | R^2 | 0.9855 | 0.9447 | 0.9665 |
| 72 h | IC_{50} ($\mu\text{g L}^{-1}$) | 23,693 | 20,102 | 19,911 |
| | IC_{50} range ($\mu\text{g L}^{-1}$) | 20,897 to 26,864 | 17,786 to 22,720 | 16,945 to 23,398 |
| | R^2 | 0.9773 | 0.9409 | 0.9779 |
| 96 h | IC_{50} ($\mu\text{g L}^{-1}$) | 15,856 | 13,399 | 12,892 |
| | IC_{50} range ($\mu\text{g L}^{-1}$) | 14,057 to 17,885 | 11,415 to 15,729 | 10,722 to 15,501 |
| | R^2 | 0.9821 | 0.9197 | 0.9719 |

4. Discussion

Stomata are the main routes for leaf transpiration, gas exchange, and controlling CO_2 uptake. Stomatal damage or closure reduces CO_2 uptake, thereby weakening photosynthesis and the photosynthetic oxygen evolution rate. Some studies show that the photosynthetic oxygen evolution rate (reflecting photosynthetic rate) determined by the conventional Oxygraph respirometers is a reliable indicator to quantify the inhibition of photosynthesis by pollutants [27]. Other studies report that Fv/Fm (reflecting efficiency and physiological status of photosynthetic organs), another well-validated indicator based on photosynthetic electron transport rate, can be detected rapidly and non-invasively by a chlorophyll fluorometer [1]. Moreover, gas exchange (characterization of photosynthetic efficiency), the third most common technique of photosynthesis research, can be mensurated by measuring CO_2 fixation efficiency. In addition, there are some in vitro physiological and biochemical methods involving extraction and isolation of photosynthetic organs. However, the above methods cannot provide spatial distribution of the bioindicators. CLSM can acquire images, but the spatial resolution is at best submicrometer resolution and in most cases cannot provide accurate concentration information of the bioindicators.

This study shows SECM provides a solution to these limitations by mapping concentration data at high spatial resolution using UMEs and precise positioning and scanning systems. The greatest advantage of SECM is its ability to probe chemical/electrochemical

information of electron and ion transfer processes at the interfaces [12]. When the probe (usually a Pt disc electrode with diameter < 25 μm) is rastered above a plane approaching the substrate, SECM is able to map out the surface topography and/or chemical redox reactions by monitoring the current perturbation. The accurate tip position and the exact current measured determine the high quality of SECM images. The principle of SECM to probe toxic effects on photosynthetic oxygen evolution is based on the role of the oxygen produced by water splitting as a mediator. The changes in the mediator concentration induced by environmental stress can be very sensitively detected as change in the current by the UME of SECM in the 'substrate-generation and tip-collection mode' [28]. Therefore, monitoring oxygen concentration profiles affords a possible pathway for direct and real-time detection of oxygen evolution response to the stress. SECM can in vivo and in situ image the cell respiration rate and plant photosynthetic oxygen evolution, which supply supplementary information for traditional liquid oxygen electrode methods.

Zhu, R.K. [12] firstly used an SECM probe to detect oxygen evolution and the changes in individual stoma structure in *Brassica juncea* (L.) Czern. cv. AC Vulcan caused by Cd stress. These limited pioneering studies by predecessors demonstrated the great potential of application of SECM in the field of ecotoxicology. In the present study, the results show that the photosynthetic oxygen evolution rate and F_v/F_m of *M. pteropus* significantly decreased with increasing 2,4-DCP concentration (Figure 3c,e). This indicates that photosynthesis of *M. pteropus* is stressed upon 96 h exposure to 2,4-DCP. The SECM data and the Clark oxygen evolution data indicate the toxicity of 2,4-DCP to the water-splitting center, while the F_v/F_m data imply that the electron transport was inhibited by 2,4-DCP on the donor side or/and on the acceptor side (Figure 3). The close values of IC_{50} between stoma center current by SECM and two conventional methods (O_2 evolution and F_v/F_m) verifies that the SECM method is a reliable method to probe the toxicity of 2,4-DCP to photosynthesis on the primary electron donor side.

In addition, the clear shape of the stoma and regular change in its structure from the SECM images show that SECM has the advantage of simultaneously mapping the topography of stomata and photosynthesis activity. Before its wide application to ecotoxicology, the protocols to ensure the reliability of SECM need to be checked with more higher plants and photosynthesis microbes exposed to more pollutants (heavy metals, saline-alkali, and compound contaminants).

The resolution of SECM mainly depends on the size and shape of the probe and the distance between the probe and the substrate, so the quality of the probe is very important to SECM imaging [29]. We suggest using high-quality UMEs with good C-V curves and proper RG values. In addition, the resolution of the SECM is determined by the parameters of the instrument (including shock resistance and thermal stability), scanning speed, appropriate electrolyte solution, whether the end face of the probe and the substrate surface are as parallel as possible, as well as the gas escape from the electrode reaction. With the continuous improvement and development of the SECM instrument itself (including the improvement of resolution) [30,31] and its combination with other measurement methods, it will also become a major development trend of ecotoxicology.

5. Conclusions

We present a novel ecotoxicological method describing the detection process based on nanoscale electrochemical mapping of photosynthetic oxygen evolution of aquatic plants by SECM. In this technology, a well-polished 10 μm diameter platinum UME was used as the SECM tip, a 0.5 mm platinum wire served as the counter electrode, and Ag/AgCl served as the reference electrode. A phosphate buffered saline (PBS, pH 6.86) solution containing 0.1 M NaHCO_3 was used as the supporting electrolyte which could provide excessive CO_2 for photosynthesis during measurement.

As shown previously, this approach can be used for simultaneous topographical and electrochemical scanning experiments of stoma oxygen emission of *M. pteropus* under 2,4-DCP stress, which indicates that SECM can be a powerful and non-invasive tool used

for ecotoxicological study. Furthermore, more ecotoxicological experimental protocols on more higher plants and more pollutants (heavy metals, other organics, saline-alkali, compound contaminants, etc.) can be carried out at a later stage.

Author Contributions: Conceptualization, N.Z. and D.Z.; methodology, N.Z. and D.Z.; software, N.Z.; validation, N.Z. and D.Z.; formal analysis, N.Z.; investigation, N.Z. and D.Z.; resources, D.Z.; data curation, N.Z.; writing—original draft preparation, N.Z. and D.Z.; writing—review and editing, D.Z.; visualization, N.Z.; supervision, D.Z.; project administration, D.Z.; funding acquisition, D.Z. All authors have read and agreed to the published version of the manuscript.

Funding: The State Key Program of National Natural Science Foundation of China (No. U1703243, No. U1503281) and Ministry of Industry-university Cooperation and Collaborative Education Program of Education of the People's Republic of China (No. 230818010207279).

Data Availability Statement: Data are available from the authors by request.

Acknowledgments: We are grateful to the reviewers for their valuable comments that significantly improved our manuscript.

Conflicts of Interest: The authors declare no conflicts of interest.

References

1. Deng, C.N.; Zhang, D.Y.; Pan, X.L.; Chang, F.Q.; Wang, S.Z. Toxic Effects of Mercury on Psi and Psii Activities, Membrane Potential and Transthylakoid Proton Gradient in *Microsorium pteropus*. *J. Photochem. Photobiol. B* **2013**, *127*, 1–7. [[CrossRef](#)]
2. Wang, S.Z.; Pan, X.L.; Zhang, D.Y. Psi Showed Higher Tolerance to Sb(V) Than Psii Due to Stimulation of Cyclic Electron Flow around Psi. *Curr. Microbiol.* **2015**, *70*, 27–34. [[CrossRef](#)] [[PubMed](#)]
3. Khan, E.A.; Ahmed, H.M.I.; Misra, M.; Sharma, P.; Misra, A.N. Nitric Oxide Alleviates Photochemical Damage Induced by Cadmium Stress in Pea Seedlings. *Phyton-Int. J. Exp. Bot.* **2022**, *91*, 959–975.
4. Ciurli, Baccio, A.; Scartazza, D.; Grifoni, A.; Pezzarossa, M.; Chiellini, B.; Mariotti, C.; Pardossi, L.A. Influence of Zinc and Manganese Enrichments on Growth, Biosorption and Photosynthetic Efficiency Ofchlorellas. *Environ. Sci. Pollut. Res.* **2021**, *28*, 46764–46780. [[CrossRef](#)]
5. Baryla, A.; Carrier, P.; Franck, F.; Coulomb, C.; Sahut, C.; Havaux, M.J.P. Leaf Chlorosis in Oilseed Rape Plants (*Brassica napus*) Grown on Cadmium-Polluted Soil: Causes and Consequences for Photosynthesis and Growth. *Planta* **2001**, *212*, 696–709. [[CrossRef](#)]
6. Mallick, N.; Mohn, F.H. Use of Chlorophyll Fluorescence in Metal-Stress Research: A Case Study with the Green Microalga *Scenedesmus*. *Ecotoxicol. Environ. Saf.* **2003**, *55*, 64–69. [[CrossRef](#)] [[PubMed](#)]
7. Yasukawa, T.; Kaya, T.; Matsue, T. Characterization and Imaging of Single Cells with Scanning Electrochemical Microscopy. *Electroanalysis* **2000**, *12*, 653–659. [[CrossRef](#)]
8. Kong, D.; Li, X.; Tang, Y.; Sui, M.; Li, J.; Ma, Y.; Wang, G.; Gu, W.; Guo, X.; Yang, M. A Highly Parallel Dtt/Mb-DNA/Au Electrochemical Biosensor for Trace Hg Monitoring by Using Configuration Occupation Approach and SECM. *Ecotoxicol. Environ. Saf.* **2022**, *234*, 113391. [[CrossRef](#)]
9. Li, Y.R.; Ning, X.M.; Ma, Q.L.; Qin, D.D.; Lu, X.Q. Recent Advances in Electrochemistry by Scanning Electrochemical Microscopy. *Trends Analyt. Chem.* **2016**, *80*, 242–254. [[CrossRef](#)]
10. Zhou, Y.; Takahashi, Y.; Fukuma, T.; Matsue, T. Scanning Electrochemical Microscopy for Biosurface Imaging. *Curr. Opin. Electrochem.* **2021**, *29*, 100739. [[CrossRef](#)]
11. Tsionsky, M.; Cardon, Z.G.; Bard, A.J.; Jackson, R.B. Photosynthetic Electron Transport in Single Guard Cells as Measured by Scanning Electrochemical Microscopy. *Plant Physiol.* **1997**, *113*, 895–901. [[CrossRef](#)] [[PubMed](#)]
12. Zhu, R.K.; Macfie, S.M.; Ding, Z.F. Cadmium-Induced Plant Stress Investigated by Scanning Electrochemical Microscopy. *J. Exp. Bot.* **2005**, *56*, 2831–2838. [[CrossRef](#)]
13. Beaulieu, I.; Kuss, S.; Mauzeroll, J.; Geissler, M. Biological Scanning Electrochemical Microscopy and Its Application to Live Cell Studies. *Anal. Chem.* **2011**, *83*, 1485–1492. [[CrossRef](#)] [[PubMed](#)]
14. Tian, N.; Tian, X.; Nie, Y.; Yang, C.; Zhou, Z.; Li, Y. Enhanced 2, 4-Dichlorophenol Degradation at pH 3–11 by Peroxymonosulfate Via Controlling the Reactive Oxygen Species over Ce Substituted 3d Mn₂O₃. *Chem. Eng. J.* **2019**, *355*, 448–456. [[CrossRef](#)]
15. Xing, L.; Liu, H.; Giesy, J.P.; Yu, H. pH-Dependent Aquatic Criteria for 2,4-Dichlorophenol, 2,4,6-Trichlorophenol and Pentachlorophenol. *Sci. Total Environ.* **2012**, *441*, 125–131. [[CrossRef](#)]
16. Yin, D.Q.; Jin, H.J.; Yu, L.W.; Hu, S.Q. Deriving Freshwater Quality Criteria for 2,4-Dichlorophenol for Protection of Aquatic Life in China. *Environ. Pollut.* **2003**, *122*, 217–222. [[CrossRef](#)] [[PubMed](#)]
17. Shi, X.; Leng, H.; Hu, Y.; Liu, Y.; Duan, H.; Sun, H.; Chen, Y. Removal of 2,4-Dichlorophenol in Hydroponic Solution by Four *Salix Matsudana* Clones. *Ecotoxicol. Environ. Saf.* **2012**, *86*, 125–131. [[CrossRef](#)]
18. Li, R.; Jin, X.; Megharaj, M.; Naidu, R.; Chen, Z. Heterogeneous Fenton Oxidation of 2,4-Dichlorophenol Using Iron-Based Nanoparticles and Persulfate System—Sciencedirect. *Chem. Eng. J.* **2015**, *264*, 587–594. [[CrossRef](#)]

19. Makevita, M.; Athauda, S.; Pahalawattarachchi, V. Development of in Vitro Sterilization Procedure for Java Fern (*Microsorium pteropus*). In Proceedings of the FAuRS-2018, Peradeniya, Sri Lanka, 27 January 2018.
20. Chun-Nuan, D.; Tao, F. Responses of Photosystem I and II Activities of *Microsorium pteropus* Blume to Pb²⁺ Toxicity. *Bangladesh J. Bot.* **2017**, *46*, 1425–1428.
21. Lan, X.Y.; Wang, J.J.; Yan, Y.Y.; Li, X.Y.; Xu, F.L. Hyperaccumulation Capacity and Resistance Physiology of *Microsorium pteropus*, an Aquatic Fern to Cadmium. *Sci. Sin. Vitae* **2017**, *47*, 1113–1123.
22. Miyoshi, S.; Kimura, S.; Ootsuki, R.; Higaki, T.; Nakamasu, A. Developmental Analyses of Divarications in Leaves of an Aquatic Fern *Microsorium pteropus* and Its Varieties. *PLoS ONE* **2019**, *14*, e0210141. [[CrossRef](#)] [[PubMed](#)]
23. Angelini, V.A.; Agostini, E.; Medina, M.I.; González, P.S. Use of Hairy Roots Extracts for 2,4-Dcp Removal and Toxicity Evaluation by *Lactuca sativa* Test. *Environ. Sci. Pollut. Res.* **2014**, *21*, 2531–2539. [[CrossRef](#)] [[PubMed](#)]
24. Angelini, V.A.; Orejas, J.; Medina, M.I.; Agostini, E. Scale up of 2,4-Dichlorophenol Removal from Aqueous Solutions Using *Brassica napus* Hairy Roots. *J. Hazard. Mater.* **2011**, *185*, 269–274. [[CrossRef](#)] [[PubMed](#)]
25. Qin, Y.; Geng, S.; Jiao, W.; Liu, Y. Deep Oxidation Degradation of Aniline Wastewater by O₃/Fe(II) Process Enhanced Using High-Gravity Technology. *Chin. J. Energetic Mater.* **2018**, *26*, 448–454.
26. Wang, S.Z.; Chen, F.L.; Mu, S.Y.; Zhang, D.Y.; Pan, X.L.; Lee, D.J. Simultaneous Analysis of Photosystem Responses of *Microcystis aeruginosa* under Chromium Stress. *Ecotoxicol. Environ. Saf.* **2013**, *88*, 163–168. [[CrossRef](#)] [[PubMed](#)]
27. Wang, Y.W.; Jiang, X.H.; Li, K.; Wu, M.; Zhang, R.F.; Zhang, L.; Chen, G.X. Photosynthetic Responses of *Oryza sativa* L. Seedlings to Cadmium Stress: Physiological, Biochemical and Ultrastructural Analyses. *BioMetals* **2014**, *27*, 389–401. [[CrossRef](#)]
28. Parthasarathy, M.; Pemaiah, B.; Natesan, R.; Padmavathy, S.R.; Pachiappan, J. Real-Time Mapping of Salt Glands on the Leaf Surface of *Cynodon dactylon* L. Using Scanning Electrochemical Microscopy. *Bioelectrochemistry* **2015**, *101*, 159–164. [[CrossRef](#)]
29. Zoski, C.G. Review-Advances in Scanning Electrochemical Microscopy (SECM). *J. Electrochem. Soc.* **2016**, *163*, 3088–3100. [[CrossRef](#)]
30. Sciutto, G.; Zangheri, M.; Prati, S.; Guardigli, M.; Mirasoli, M.; Mazzeo, R.; Roda, A. Immunochemical Micro Imaging Analyses for the Detection of Proteins in Artworks. *Top. Curr. Chem.* **2016**, *374*, 32–59. [[CrossRef](#)]
31. Junjie, Z.; Tong, Z.; Jinxin, L.; Wenxuan, F.; Fei, L. Recent Advances of Scanning Electrochemical Microscopy and Scanning Ion Conductance Microscopy for Single-Cell Analysis. *Curr. Opin. Electrochem.* **2020**, *22*, 178–185.

Disclaimer/Publisher's Note: The statements, opinions and data contained in all publications are solely those of the individual author(s) and contributor(s) and not of MDPI and/or the editor(s). MDPI and/or the editor(s) disclaim responsibility for any injury to people or property resulting from any ideas, methods, instructions or products referred to in the content.